https://doi.org/10.5194/egusphere-2026-2664
Preprint. Discussion started: 11 June 2026

A New Proposal for Optimizing Maximum Hydrological Events Fitting with Flexible TCEV Distribution

Liangyu Ta[1,2], Javier Valdes-Abellan[2], Chen Yu[1,3], Zhenhong Li[1,3]

[1]State Key Laboratory of Loess Science, Chang'an University, Xi'an 710054, China
[2]Department of Civil Engineering, University of Alicante, Alicante 03080, Spain
[3]College of Geological Engineering and Geomatics, Chang'an University, Xi'an 710054, China

Correspondence to: Chen Yu (chen.yu@chd.edu.cn)

Abstract. Accurate characterization of extreme hydrological events is critical for flood risk assessment and hydraulic engineering design, particularly in the high-value cumulative distribution function (CDF, F(x)) range that governs design extremes. Hydrological records often consist of mixed populations of ordinary and extreme events, leading to a pronounced "dog-leg effect" that limits the applicability of conventional extreme-value distributions such as the Gumbel and Log-Pearson Type III. Although the Two-Component Extreme Value (TCEV) distribution is conceptually well suited to such mixed populations, its practical application is constrained by subjective parameter initialization, uniform weighting schemes that underrepresent right-tail extremes, and evaluation metrics with limited tail sensitivity. In this study, we propose a new fitting method for the TCEV distribution, SR-MWS, which uses piecewise linear fitting for stable initial parameters, right-tail-oriented weighting for extreme events, and a partitioned scoring framework to evaluate global and tail performance. The results of the hydrological dataset indicate that SR-MWS consistently outperforms existing TCEV estimation methods in accuracy and robustness. Further experiments based on simulated data show that this method achieves better global fitting performance while maintaining tail accuracy comparable to the Peaks-Over-Threshold (POT) method, and is significantly better than generalized extreme value (GEV) and Gumbel distributions in capturing extremes. By reducing subjectivity and enhancing robustness, the proposed method provides an automated framework for extreme-event modeling applicable to other mixed-population extreme-value problems.

1 Introduction

Heavy precipitation and flood events occur when rainfall intensity exceeds soil infiltration capacity and surface runoff surpasses river channel conveyance. This phenomenon ranks among the most important natural hazards regarding economic losses and human fatalities, as illustrated by the 29 October 2024 event in Spain, which caused more than 220 deaths (Galvez-Hernandez et al., 2025; Mahmood et al., 2017). Flood hazard is not limited to any specific area or climate, but represents a global hazard affecting diverse climatic and geographic settings worldwide (Rentschler et al., 2022). Consequently, accurately characterizing extreme rainfall and flood behaviour is a critical foundation not only for hydrological design and infrastructure planning, but also for probabilistic risk assessment frameworks that underpin flood hazard mapping, insurance pricing, and climate adaptation strategies.

https://doi.org/10.5194/egusphere-2026-2664
Preprint. Discussion started: 11 June 2026

A wide range of methods exists to analyse extreme hydrological events, with probabilistic modelling being one of the most widely adopted approaches because it directly links observed records to design quantiles for given return periods (Fuller Weston, 1914; Merz and Blöschl, 2008). However, the performance of probabilistic modelling is highly dependent on the type of the population distribution and the basis for parameter estimation (Rossi et al., 1984). Traditional probability methods can be divided into two categories. The first type is usually based on the generalized extreme value (GEV) distribution and its special case Gumbel distribution, modeling the annual or seasonal maximum under the assumption of independent and identically distributed (Clarke, 2002; Gumbel, 1941). This type of model is widely used due to its theoretical foundation and simple form, but its dependence on a single distribution limits its ability to capture mixed hydrological processes. The second type is the Peak-Over-Threshold (POT) method based on Generalized Pareto Distribution (GPD), which models events that exceed a predefined threshold and is particularly effective in characterizing tail behaviour (Davison and Smith, 1990; Pickands, 1975). However, the POT method is highly sensitive to threshold selection and cannot provide a complete explicit expression of the distribution, often resulting in inconsistencies between tail fitting and overall distribution representation. In addition, some empirical and semi-empirical distributions, such as the Log-Pearson Type III (Stedinger et al., 1993; Vogel Richard and Wilson, 1996) distribution , as well as regional empirical formulations such as SQRT-ET MAX (Etoh et al., 1987; Senent-Aparicio et al., 2023), have also been widely adopted in engineering practice.

A major challenge for the abovementioned methods arises in regions where annual maximum precipitation or flood records reflect mixed flood-generating mechanisms. In these settings, probability plots often exhibit the so-called “dog-leg effect” or “separation phenomenon”, in which observations display two distinct regimes corresponding to frequent, ordinary events and rare, extraordinary extremes (Matalas et al., 1975; Potter, 1958). This behaviour is not merely a statistical artifact but reflects fundamentally different atmospheric processes governing ordinary and extraordinary events. This separation challenges the fundamental assumption of homogeneous extreme-value populations and represents a key source of bias in conventional frequency analyses based on single-distribution models.

Beyond the presence of mixed populations, the assumption of stationarity under extreme hydrological conditions is increasingly being challenged by climate change (Fowler et al., 2021; Papalexiou and Montanari, 2019). The changes in atmospheric circulation patterns and flood generation mechanisms have been shown to alter the statistical characteristics of extreme events, particularly the distribution skewness and tail behaviour (Moustakis et al., 2021). De Luca et al. (2024) demonstrated that climate driven extreme rainfall changes are closely related to changes in distribution skewness, which in turn affects the estimation of high recurrence quantiles. From this perspective, the separation phenomenon in the annual maximum value sequence can be understood as both a manifestation of mixed populations and a signal of hydrological process evolution under changing climate conditions. This further increases the challenge of accurately representing the

https://doi.org/10.5194/egusphere-2026-2664
Preprint. Discussion started: 11 June 2026

right-tail of the distribution, particularly under conditions where rare extreme events have become more influential and unpredictable.

To address this issue, the Two-Component Extreme Value (TCEV) distribution (Rossi et al., 1984) was introduced to represent annual maxima as a mixture of two exponential components and has since been applied in a variety of hydrological studies (Cannarozzo et al., 1995; Ferro and Porto, 2006; Boni et al., 2006; Escalante-Sandoval and Reyes-Chávez, 2004). However, existing studies reveal several fundamental limitations in the practical application of the TCEV distribution. The determination of initial parameters often relies on manual intervention, introducing subjectivity and analyst-dependent variability that can compromise the robustness of parameter estimation (Campos-Aranda, 2021). Moreover, parameter estimation is commonly performed using uniform weighting and global goodness-of-fit criteria (Francés, 1998), causing frequent events to dominate the fitting process and obscuring biases in the right-hand tail that are critical for rare-event quantile estimation.

In this study, we propose a refined TCEV fitting framework that restores the influence of extreme events in frequency analysis while maintaining a fully automated and objective estimation workflow. This workflow establishes a verifiable and transferable framework aimed at enhancing the accuracy of extreme-event quantification. As such, the proposed framework provides a methodological foundation for more credible regional frequency analysis and for the reassessment of existing hydraulic infrastructure safety in regions affected by mixed flood-generating mechanisms.

2 Method

2.1 Basic background of the TCEV distribution

The TCEV distribution is developed to analyze maximum hydrological events generated by two distinct physical processes. Unlike mixture models, it avoids assigning explicit weights to each process. Instead, it models the annual occurrence of hydrological events, including ordinary and extreme processes, as random variables. As demonstrated by Fiorentino et al. (1987), the combined effect of these two processes results in a specific distribution, offering a framework for understanding hydrological risk based on these underlying stochastic processes.

As Rossi et al. (1984) stated, the TCEV accounts for outliers and high skewness in the right-tail of the observed cumulative probabilities by recognizing that the data originate from a mixture of populations. In its fundamental form, the TCEV distribution models ordinary and extraordinary events as arising from two independent Gumbel populations, and the Cumulative Distribution Function (CDF) can be expressed as a product of two Gumbel equations (Gumbel, 1941, 2004):

$$F_{TCEV}(x) = F_{GUMBEL1}(x) \cdot F_{GUMBEL2}(x) = exp\left(-exp\left(-\alpha_1 \cdot (x - \beta_1)\right)\right) \cdot exp\left(-exp\left(-\alpha_2 \cdot (x - \beta_2)\right)\right), \quad (1)$$

https://doi.org/10.5194/egusphere-2026-2664
Preprint. Discussion started: 11 June 2026

where α_1 and β_1 are the parameters that govern the left-tail part of the data (corresponding to the ordinary events) and α_2 and β_2 are the parameters governing the right-tail part of the data (corresponding to the extraordinary events).

2.2 Existing TCEV estimation frameworks

Numerous TCEV parameter estimation strategies for Eq. (1) have since been proposed, including maximum likelihood inference (Rossi et al., 1984), frameworks incorporating historical floods (Francés, 1998), entropy-based estimation (Fiorentino et al., 1987), and simulation-driven or regionalized procedures (De Luca and Napolitano, 2023). This section briefly outlines three state-of-art methods.

The first optimization method, named TCEV-IML, is based on a continuous substitution process (Campos-Aranda, 2021). This method uses a specific update formula to calculate new parameters and monitor the logarithmic maximum likelihood function to gradually optimize the TCEV parameters until convergence. The second optimization method, named TCEV-MOF, aims to maximize an objective function (Campos-Aranda, 2021), which is the negative version of the logarithmic maximum likelihood function. It employs the Rosenbrock (Rosenbrock, 1960) algorithm to find the optimal parameters. The third optimization method, named TCEV-MCS, solves the TCEV parameters through statistical tests. It estimates the "ordinary event" parameters via the maximum likelihood method, while identifying the "extreme event" parameters using the Monte Carlo method (Kottegoda and Rosso, 2008). The detailed procedure is described in De Luca and Napolitano (2023).

In summary, TCEV-IML employs continuous substitution, TCEV-MOF leverages the Rosenbrock algorithm to maximize the maximum likelihood function, and TCEV-MCS combines statistical tests with Monte Carlo simulations. Although these methods differ in their optimization strategies, they typically rely on global fitting criteria that assign equal importance throughout the distribution. In the context of climate change, the skewness and tail characteristics of extreme value distributions are evolving (De Luca et al., 2024), which further increases the complexity of parameter estimation. Therefore, there is a growing need for an estimation framework that can effectively characterize right-tail behaviour. This paper compares the proposed method with these three established methods to validate its effectiveness and robustness.

2.3 A Slope-Ratio guided Multi-Weighting Scheme (SR-MWS) method

The proposed SR-MWS method can be divided into four steps, including data processing and empirical CDF calculation, TCEV applicability diagnosis via slope-ratio criterion, nonlinear optimization of TCEV parameters with multi-weighting scheme, and selecting the optimal scheme by a partitioned scoring framework. The process is illustrated as a flow chart in Fig. 1.

https://doi.org/10.5194/egusphere-2026-2664
Preprint. Discussion started: 11 June 2026

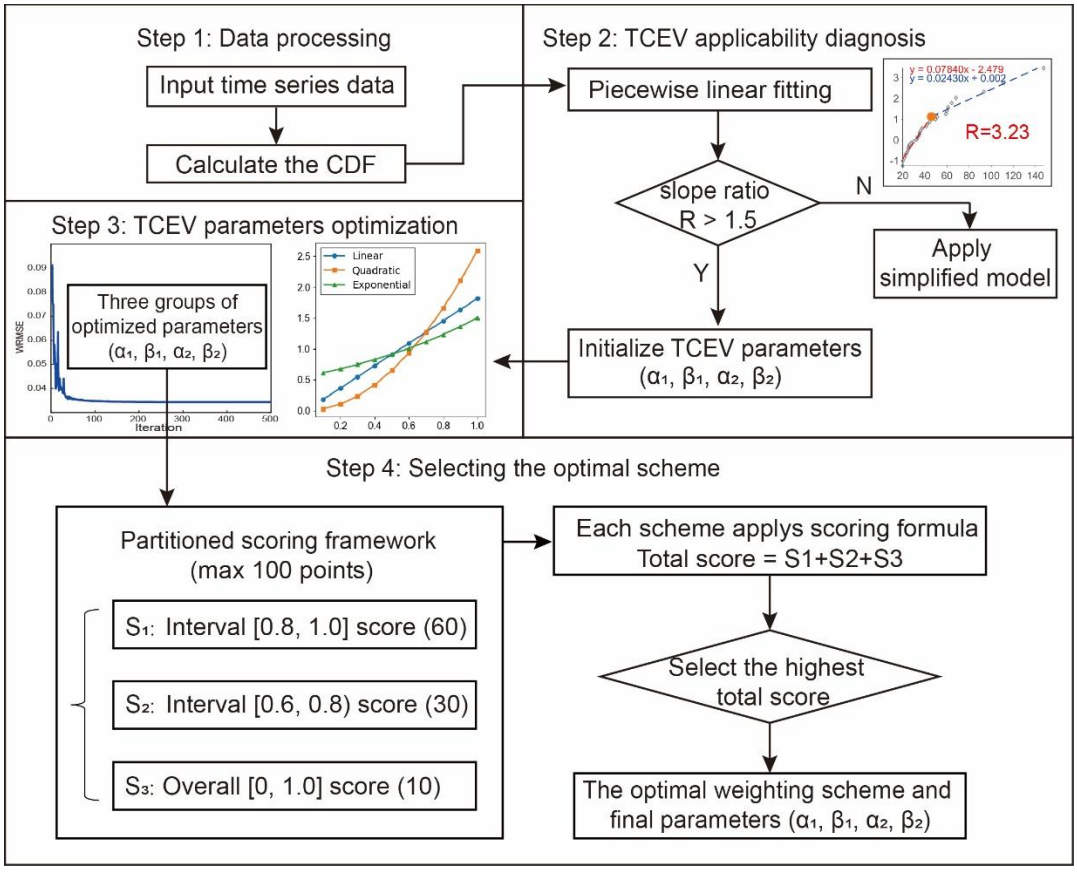

Figure 1: Flowchart of the SR-MWS method.

2.3.1 Data processing and empirical CDF calculation

The input data represent annual maximum series (either precipitation or flow series). The Weibull formula (Weibull, 1939) is employed to calculate the CDF from observations.

$$F(x_i) = \frac{i}{N+1}, \tag{2}$$

where, i is the rank of the data point (sorted in ascending order) and N is the total number of observations. Other alternatives can be found in scientific literature (Blom, 1958; Gringorten, 1963; Cunnane, 1978; Hazen, 1914), and a review of them can be found in Helsel and Hirsch (2002). However, regardless of the alternative selected to calculate the CDF, the 'dog-leg effect' is going to remain. It does not affect the aim of the present work, so we have selected the simplest and most mainstream approach.

https://doi.org/10.5194/egusphere-2026-2664
Preprint. Discussion started: 11 June 2026

2.3.2 TCEV applicability diagnosis via slope-ratio criterion

A key property of the Gumbel distribution is that its CDF, $F_{GUMBEL}(x)$, can be linearized by applying a double negative logarithmic transformation. Applying this transformation yields a new variable $\mathcal{Z}$, which plots as a straight line:

$$\mathcal{Z} = -ln\left(-ln\left(F_{GUMBEL}(x)\right)\right) = \alpha x - \alpha\beta \,, \tag{3}$$

here, α is the slope parameter and must always be positive. $(-\alpha\beta)$ is the intercept value of the line at the origin.

Under the transformation defined by Eq. (3), the TCEV distribution is characterized by two linear segments. We set a minimum segment length (bpmin = 3) to ensure sufficient data points for reliable fitting. The optimal breakpoint (xybp) was determined by minimizing the Root Mean Square Error (RMSE) of the bilinear model through an iterative search. This identifies the threshold where the slope transitions between ordinary and extreme events. After the piecewise linear fitting stage, the whole dataset is split into two defined parts,

$$\begin{cases} \mathcal{Z}_1 = a_1 x + c_1 \ (lower\ segment) \\ \mathcal{Z}_2 = a_2 x + c_2 \ (upper\ segment) \end{cases}, \tag{4}$$

The four linear parameters (a_1, c_1, a_2, c_2) obtained above are then used to calculate the four initial parameters for the TCEV distribution (Eq. (5)).

$$\begin{cases} \alpha_1 = a_1 \\ \beta_1 = -\frac{c_1}{a_1} \\ \alpha_2 = a_2 \\ \beta_2 - \frac{c_2}{a_2} \end{cases}, \tag{5}$$

A preliminary TCEV distribution can be constructed by directly using initial parameters (α_1, β_1, α_2, β_2). This approach reduces the probability of falling into equifinality problems (Valdes-Abellan et al., 2018), which arise when parameters from two individually fitted Gumbel distributions are combined. Although the TCEV parameters obtained by directly combining the two Gumbels is suboptimal, the shape parameters from both Gumbels are useful for analyzing the uniqueness and uncertainty of the final parameters (Beven and Binley, 1992).

To objectively evaluate the effectiveness of this piecewise linear analysis and determine the applicability of the TCEV distribution, we employ a slope-ratio criterion ($R = {}^{a_1}/_{a_2}$), where a_1 and a_2 represent the slopes of the first and second segments, respectively. In this study, we rejected the application of the TCEV distribution when the difference between the two segments was not sufficiently clear. The SR-MWS method is applied only when the slope ratio ($R > 1.5$) confirms the proper growth pattern and supplementary evidence supports bimodal behaviour. This ensures SR-MWS method is used for

https://doi.org/10.5194/egusphere-2026-2664
Preprint. Discussion started: 11 June 2026

datasets that clearly show two-phase extreme value traits and avoids overcomplicating things when simpler methods can accurately capture the data's behaviour.

2.3.3 Nonlinear optimization of TCEV parameters with MWS

This paper introduces a multi-weighting scheme (MWS) designed to more accurately characterize the right-tail of the distribution, a priority given that under climate change extreme events are becoming both more influential and uncertain. We evaluated three different weighting schemes to improve the fit for extreme values (i.e., high F(x)). The core idea was to assign greater importance to these points during optimizing by incorporating weights into the RMSE minimization framework. This leads to a weighted RMSE (WRMSE) (Eq. (6)) where the standard RMSE is modified to emphasize specific regions of the distribution (Wojtczak et al., 2024; Wojtczak et al., 2020). The WRMSE is calculated as:

$$WRMSE = \sqrt{\frac{1}{N}\sum_{i=1}^{N}\left(y_i - y_{ref}\right)^2 * w_j}\ (j = 1, 2, 3)\ , \tag{6}$$

where N is the number of data points, y_i and y_{ref} are the fitted and empirical CDF values, respectively, and w_j denotes the three weighting schemes, including linear weighting according to the CDF (Eq. (7)), quadratic weighting according to the CDF (Eq. (8)), and exponential weighting according to the CDF (Eq. (9)).

$$w_1 = F(x)/mean(F(x))\ , \tag{7}$$

$$w_2 = \left(F(x)\right)^2/mean(\left(F(x)\right)^2)\ , \tag{8}$$

$$w_3 = e^{F(x)}/mean(e^{F(x)})\ , \tag{9}$$

The normalization of the weighting schemes (as shown in Fig. 2) serves two key purposes. First, it ensures that the average weight across all data points is approximately 1, preserving the overall scale of the target statistic WRMSE and preventing numerical instability during optimization. Second, it preserves the differences in relative importance between data points. As visualized in Fig. 2, the normalized schemes clearly demonstrate how different weighting schemes distribute importance relative to the average level, showing particularly the relative emphasis in the high F(x) region (extreme events).

https://doi.org/10.5194/egusphere-2026-2664
Preprint. Discussion started: 11 June 2026

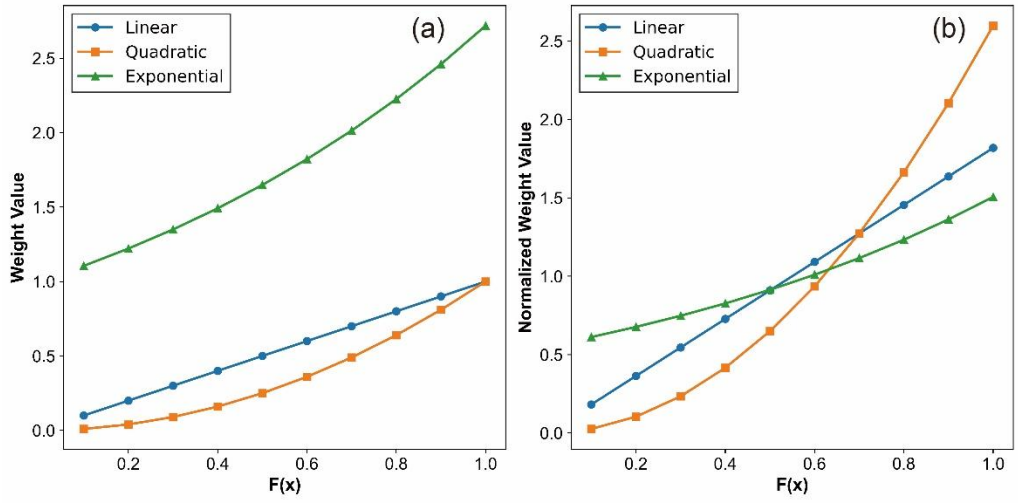

Figure 2: Comparison of weighting schemes before and after normalization. (a) Raw weighting scheme. (b) Normalized weighting scheme.

Each weighting scheme emphasizes the importance of extreme events to a different degree. The optimization was carried out through an iterative process in which the parameters (α_1, β_1, α_2, β_2) were repeatedly adjusted to minimize the WRMSE. This iterative refinement progressively improved the match between the fitted TCEV distribution and the observations. As the three proposed weighting schemes focus more on the high F(x) values, the application of any of them during optimization improves the fit in the right-tail of the distribution at the cost of worsening fit in the left-tail. In this study, we considered that a homogeneous weighting scheme, which assigns the same importance to all data, was not adequate, as it results in a poorer fit in the domain of high F(x) values, which is most critical for hydrological design.

2.3.4 Selecting the optimal scheme by a partitioned scoring framework

Through nonlinear optimization, we obtained three sets of refined TCEV distribution parameters. To identify the optimal weighting scheme and its parameters (α_1, β_1, α_2, β_2) for achieving high accuracy in the medium-to-high F(x) range, we implemented a structured scoring framework. This framework divided the F(x) range into five consecutive intervals ([0, 0.2), [0.2, 0.4), [0.4, 0.6), [0.6, 0.8), and [0.8, 1.0]) along with the overall interval [0, 1.0]. The RMSE of each weighting scheme was calculated for every interval. These RMSE values were used not only to select the optimal weighting scheme but also to further analyze the performance of different TCEV distribution fitting methods across the defined intervals. These intervals correspond to progressively higher return periods, with the interval [0.6, 0.8) representing events with return periods of approximately 2.5 to 5 years, and the interval [0.8, 1.0] capturing more extreme events with return periods exceeding 5 years, extending to 200 years at F(x)=0.995 and beyond. Based on this, we defined three key evaluation areas to guide the final selection.

https://doi.org/10.5194/egusphere-2026-2664
Preprint. Discussion started: 11 June 2026

We set the high-value interval [0.8, 1.0] as the main area of focus and assigned it a maximum of 60 points. The adjacent interval [0.6, 0.8) was designated as the secondary focus area, and was allocated 30 points to it. The overall performance across the entire dataset [0, 1.0] was also considered and was assigned 10 points for it. To calculate the score of a weighting scheme within each evaluation interval, we used the normalized ratio method. Thus, the scheme with the best performance (the lowest RMSE) in a given domain received the maximum points allocated to that domain. The scoring formula is as follows:

$$S_k = P_k \times \frac{RMSE_{min,k}}{RMSE_{w,k}}, \tag{10}$$

where, S_k is the score awarded to the weighting scheme for the evaluation interval k. P_k is the maximum points allocated to an interval k (i.e., 60, 30, or 10 points). $RMSE_{min,k}$ is the lowest RMSE value achieved by any weighting scheme within the interval k. $RMSE_{w,k}$ is the RMSE of the weighting scheme w being evaluated in the interval k.

The weighting scheme with the highest aggregate score across all three intervals was selected as optimal, thereby determining its corresponding parameters (α_1, β_1, α_2, β_2). The TCEV distribution fitting curve, identified through this structured and objective framework, accurately captured the right-tail of the data, especially at high F(x) values. Consequently, the proposed SR-MWS method provides a robust and reliable basis for estimation and can accurately predict the intensity values and return periods of extreme hydrological events that fall outside the historical record.

2.4 Benchmark methods

To ensure fairness and comprehensiveness in the evaluation, this paper compares the proposed framework with three widely used benchmark methods, including the GEV distribution, the Gumbel distribution, and the POT method. For the GEV and Gumbel methods, parameters are estimated using maximum likelihood estimation (MLE), which is widely applied in hydrological frequency analysis due to its high statistical efficiency and consistency (Coles et al., 2001). The Gumbel distribution is a special case of the GEV distribution when the shape parameter equals zero. For the POT method, the threshold is set at the 80th percentile of the observed data, and exceedances are modeled using a GPD, whose parameters are also estimated via MLE. All benchmark methods are implemented within a unified framework, using the same dataset and evaluation metrics to ensure comparability.

3 Dataset

3.1 Hydrological data

We selected several datasets, drawn from already published research studies and directly from weather stations (like Alicante weather station), to validate the proposed SR-MWS method. These datasets, shown in Fig. 3, cover a wide range of

https://doi.org/10.5194/egusphere-2026-2664
Preprint. Discussion started: 11 June 2026

240 recording periods from 31 to 155 years. Cases 7 and 8 were specifically chosen to demonstrate the usefulness of the piecewise linear fitting described in Sect. 2.3.2. The datasets include both flood flow measurements (m^3/s) and precipitation records (mm). This multi-type data assessment approach transcends the limitations of a single data source, making the parameter estimation results more practically applicable and reliable.

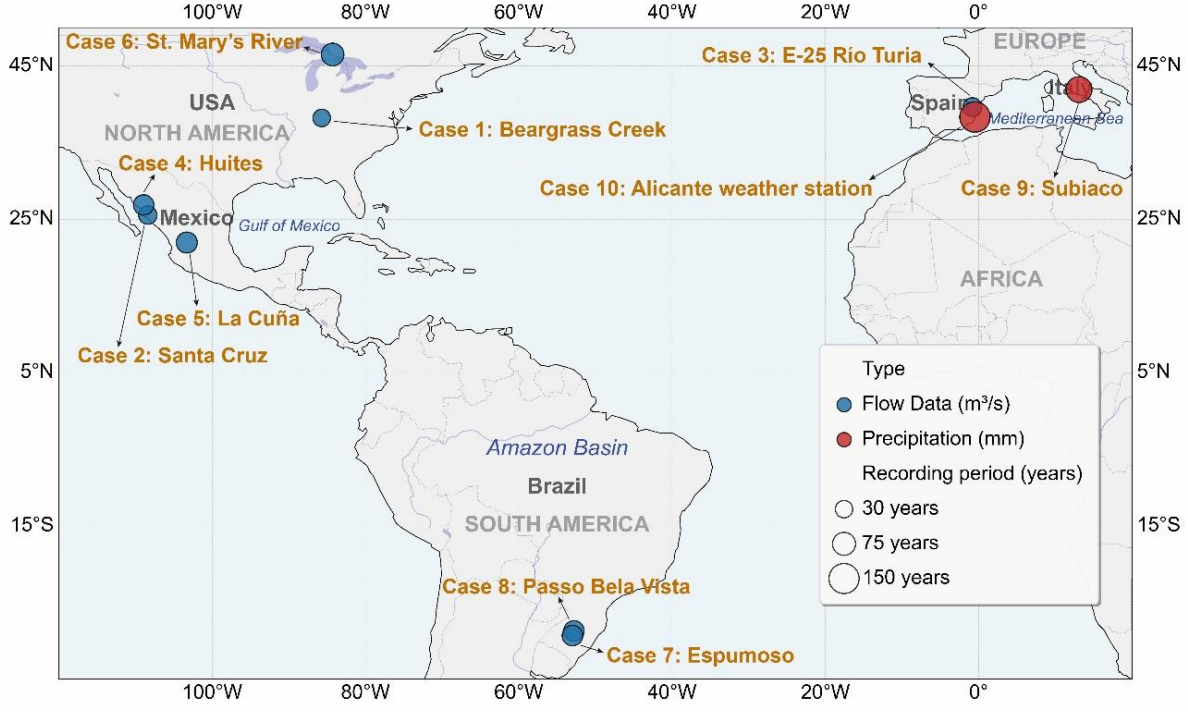

245 **Figure 3: Location of cases (station/river) with corresponding flow, precipitation, and recording periods. Case 1: Beargrass Creek (Haan et al., 1994); Case 2: Santa Cruz (Molina-Aguilar et al., 2018); Case 3: E-25 Río Turia (Francés, 1995); Case 4: Huites (Aranda, 1999); Case 5: La Cuña (Gómez et al., 2010); Case 6: St. Mary's River ; Case 7: Espumoso (Clarke, 2002); Case 8: Passo Bela Vista (Clarke, 2002); Case 9: Subiaco (De Luca and Napolitano, 2023); Case 10: Alicante weather station.**

The TCEV parameter values for the datasets, obtained using the existing estimation methods described in Sect. 2.2, are 250 summarized in Table 1. We systematically applied mathematically equivalent transformations to these parameters to unify findings from the literature into the expression form adopted in this study. For Case 10, corresponding reference data were unavailable, so it was analyzed only with the method proposed in this paper.

Table 1: TCEV fitting parameters for seven cases from different estimation methods.

Cases	Methods	α_1	β_1	α_2	β_2
1	TCEV-IML	0.063	39.419	0.0216	-11.291
	TCEV-MOF	0.123	27.918	0.023	-19.230
2	TCEV-IML	0.003	633.791	0.0005	-3129.644
	TCEV-MOF	0.004	729.148	0.0006	-1274.060

https://doi.org/10.5194/egusphere-2026-2664
Preprint. Discussion started: 11 June 2026

3	TCEV-IML	0.026	61.386	0.0007	-2775.673
	TCEV-MOF	0.027	60.849	0.0009	-1913.150
4	TCEV-IML	0.002	1221.718	0.0002	-5227.123
	TCEV-MOF	0.002	1445.455	0.0002	-6417.100
5	TCEV-IML	0.006	257.179	0.001	-1009.472
	TCEV-MOF	0.006	280.490	0.001	-1157.490
6	TCEV-IML	0.010	308.361	0.0056	-63.048
	TCEV-MOF	0.010	315.582	0.007	165.375
9	TCEV-MCS	0.066	59.756	0.0219	-45.407

3.2 Simulated data

We evaluate the performance of the proposed method under controlled conditions and compare it with the benchmark methods described in Sect. 2.4. To this end, simulated datasets were generated from several distributions commonly used in hydrological frequency analysis, including TCEV, GEV, lognormal distribution, exponential distribution, and Pareto distribution. These distributions cover a wide range of statistical features, particularly in terms of skewness and tail behaviour. The sample size for each dataset was randomly selected from the set {30, 50, 100, 200} to cover both small and large sample scenarios commonly encountered in hydrological applications. For each dataset, the theoretical CDF was computed according to Eq. (2) and used as a reference for evaluation. To ensure statistical robustness, 200 simulated datasets were generated independently. This simulation framework enables comparison between the proposed method and the benchmark methods in Sect. 2.4 under diverse conditions, with evaluation focusing on both overall fitting accuracy and tail modeling capability.

4 Results

4.1 TCEV applicability diagnosis

Based on the piecewise linear fitting analysis, the slope-ratio criterion R was used to evaluate the applicability of the TCEV distribution (see Sect. 2.3.2). The results of this diagnosis for the ten cases are presented in Fig. 4. It is clear that in most cases, the R values exceed 1.5. In contrast, Cases 7 and 8 yielded R values below 1.5 (0.28 and 0.5, respectively), suggesting that the TCEV distribution may not be the optimal choice for these particular datasets. Therefore, the subsequent analysis was continued only with the remaining eight cases that met the criterion.

https://doi.org/10.5194/egusphere-2026-2664
Preprint. Discussion started: 11 June 2026

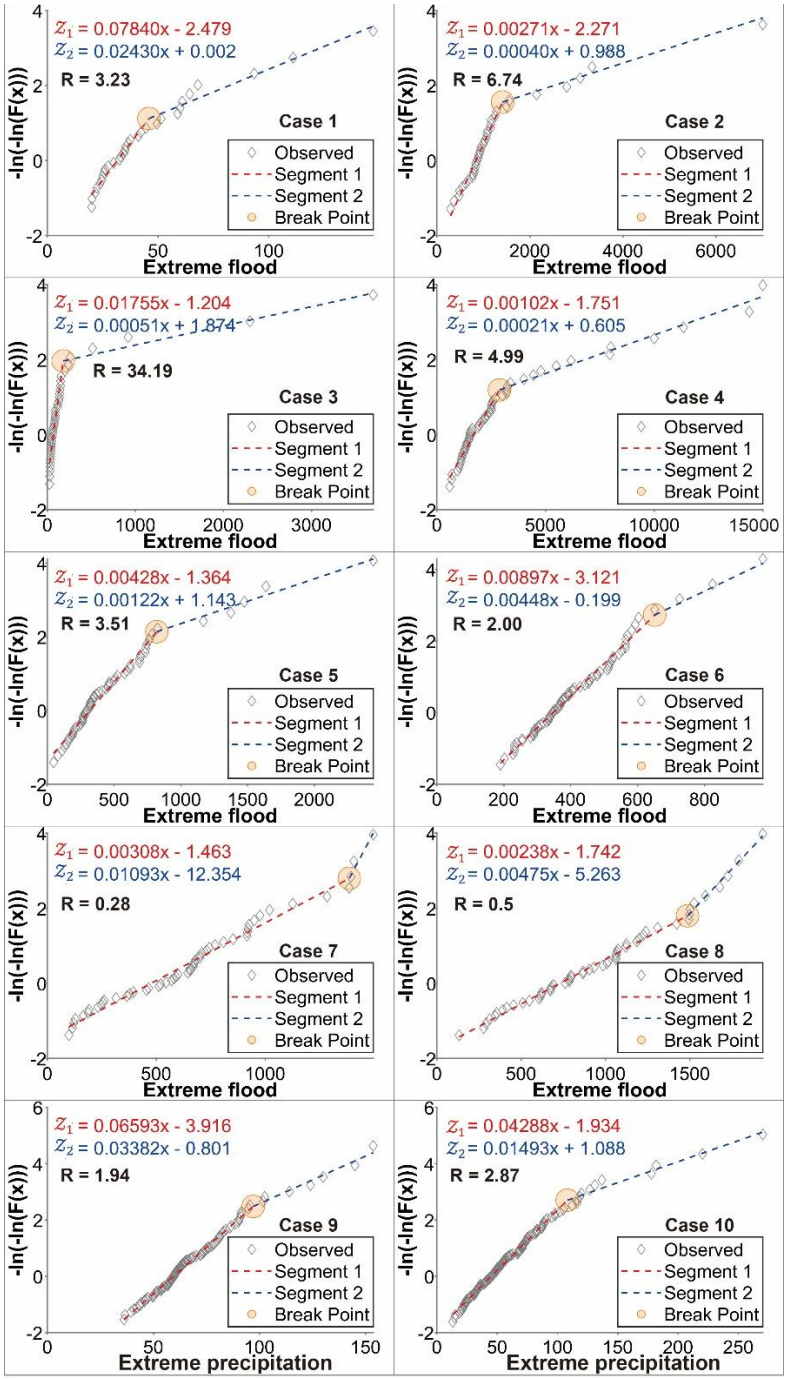

Figure 4: Piecewise linear regression analysis of extreme flood (Cases 1-8) and extreme precipitation (Cases 9-10) across ten cases. The vertical axis represents the transformed value of the F(x), i.e., -ln(-ln(F(x))). The horizontal axis denotes the magnitude of extreme flood (m^3/s) or precipitation (mm) events. Observed points are depicted as diamonds, while the two segments of the piecewise linear fitting are shown as dashed lines (lower segment in red, upper segment in blue). The break point between segments is marked by a circle. Each segment is accompanied by its respective regression equation ($\mathcal{Z}_1$ and $\mathcal{Z}_2$) in the form $\mathcal{Z} = a \cdot x + b$, where a is the slope and b is the intercept. *R* indicates the TCEV applicability.

https://doi.org/10.5194/egusphere-2026-2664
Preprint. Discussion started: 11 June 2026

According to our proposed criteria, these datasets should be set aside in favor of alternative modeling approaches, such as linear fitting or others, which may better capture the underlying patterns. This recommendation is consistent with previous research by Clarke (2002), who analyzed the same dataset using General Linear Models (GLM) combined with a Gumbel distribution.

4.2 Optimizing TCEV parameters through WRMSE minimization

After obtaining the initial parameters through piecewise linear fitting, we optimized the TCEV distribution parameters by minimizing the WRMSE using multiple weighting schemes that assign greater weight to right-tail observations. The comparison of the three weighting schemes across eight representative cases is shown in Fig. 5, reflecting their effects on TCEV parameter estimation. Starting from identical initial values, the parameters under all weighting schemes progressively stabilized with increasing iterations, indicating convergence. This convergence was accompanied by a substantial reduction in WRMSE, with decreases exceeding 70% in most cases.

The three weighting schemes differ in their performance across cases. To identify the optimal weighting scheme, we conducted a comprehensive evaluation using the scoring framework in Sect. 2.3.4. The scheme with the highest score is regarded as the optimal choice, and its corresponding TCEV distribution parameters are summarized in Table 2. As illustrated in Fig. 6 and Fig. 7, the quadratic weighting scheme achieved the highest overall score in six cases (Cases 1, 2, 3, 5, 6 and 10), establishing it as the optimal choice. The linear scheme performed best in Case 4, while the exponential scheme was optimal in Case 9.

Table 2: The final selected parameters (α_1, β_1, α_2, β_2).

Case	α_1	β_1	α_2	β_2
1	0.092	26.144	0.0209	-22.465
2	0.005	807.508	0.0004	-2553.194
3	0.019	52.440	0.0004	-4729.926
4	0.001	1362.312	0.0002	-5874.290
5	0.005	253.716	0.0011	-1254.509
6	0.009	335.271	0.0085	35.376
9	0.100	50.410	0.0499	48.464
10	0.044	43.454	0.0059	-514.482

https://doi.org/10.5194/egusphere-2026-2664
Preprint. Discussion started: 11 June 2026

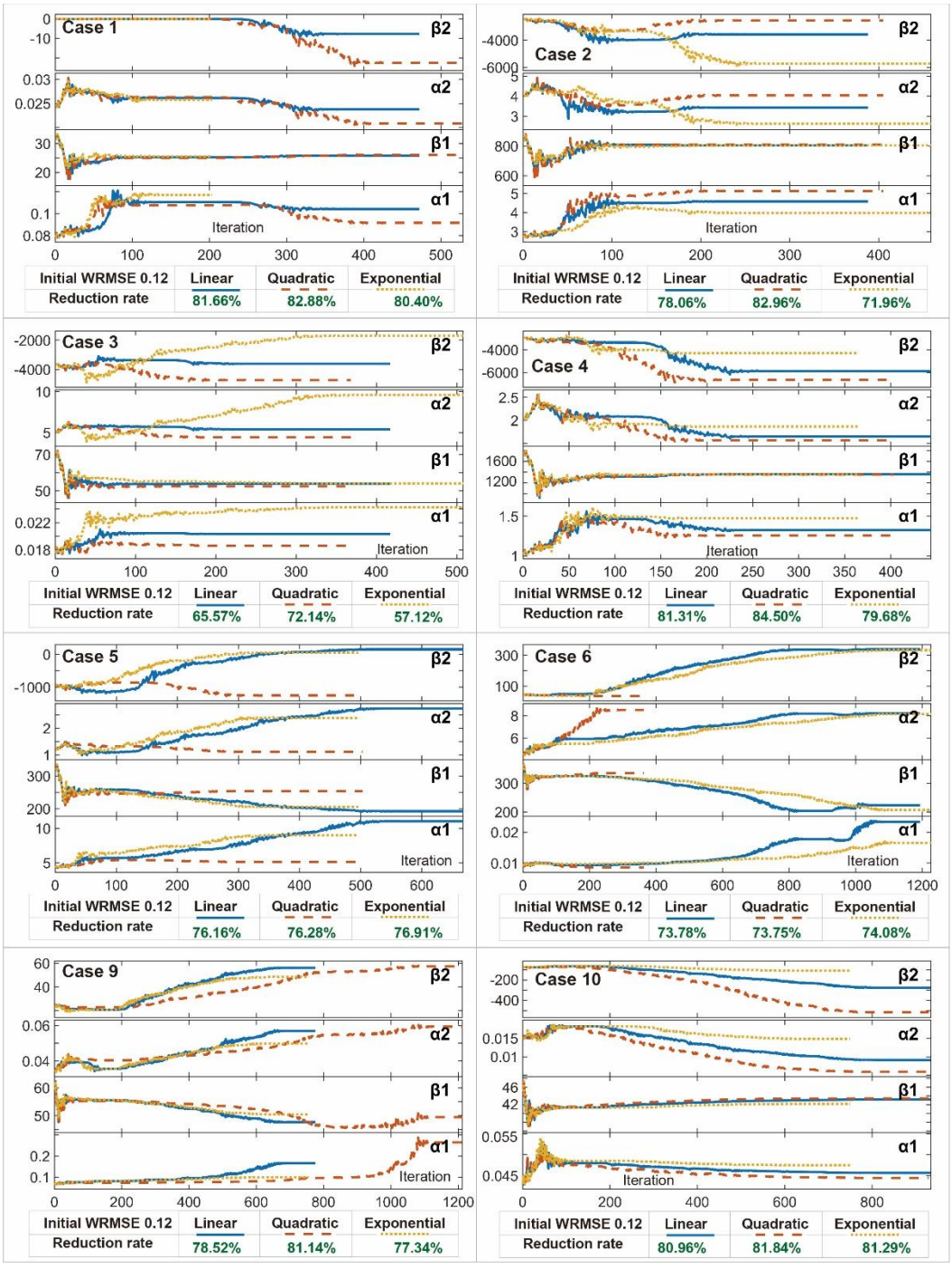

Figure 5: TCEV distribution parameters evolution and WRMSE reduction rate comparison across cases with different weighting schemes. Each case contains four sub-graphs. In each subgraph, the horizontal axis represents the number of iterations, and the vertical axis represents the value of the corresponding parameter. The blue, orange, and yellow lines represent the linear, quadratic, and exponential weighting schemes, respectively. At the bottom of each case, the initial WRMSE value and the WRMSE reduction rates under the three weighting schemes are provided.

https://doi.org/10.5194/egusphere-2026-2664
Preprint. Discussion started: 11 June 2026

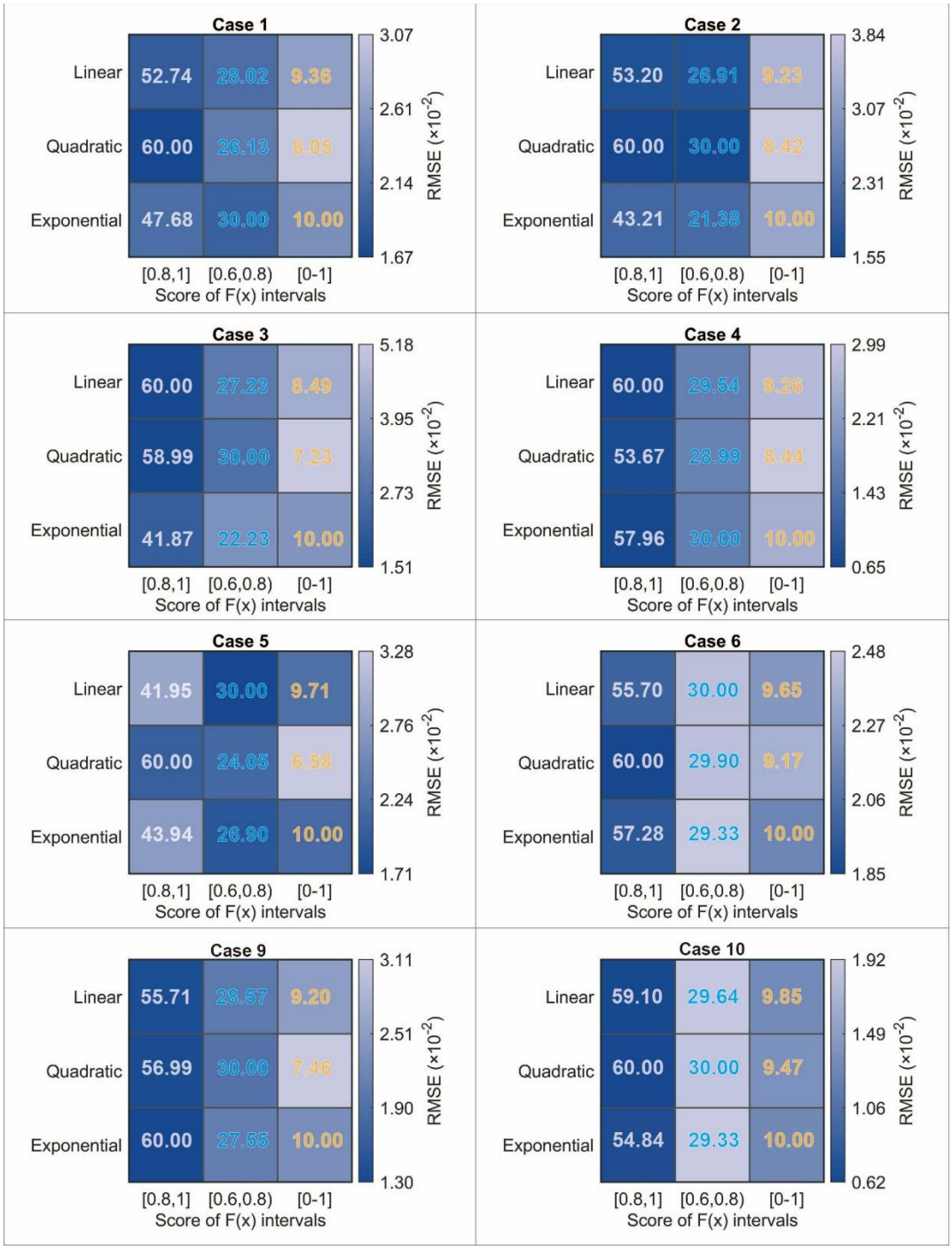

Figure 6: Performance comparison of the weighting schemes (linear, quadratic, and exponential) across F(x) intervals. In each heatmap, rows correspond to the weighting schemes, and columns correspond to the intervals of F(x), namely [0.8, 1], [0.6, 0.8), and [0, 1.0]. The color gradient represents the magnitude of the RMSE, with darker shades indicating lower RMSE values. The value in each grid cell represents the performance score (derived from the RMSE) calculated based on our proposed framework.

https://doi.org/10.5194/egusphere-2026-2664
Preprint. Discussion started: 11 June 2026

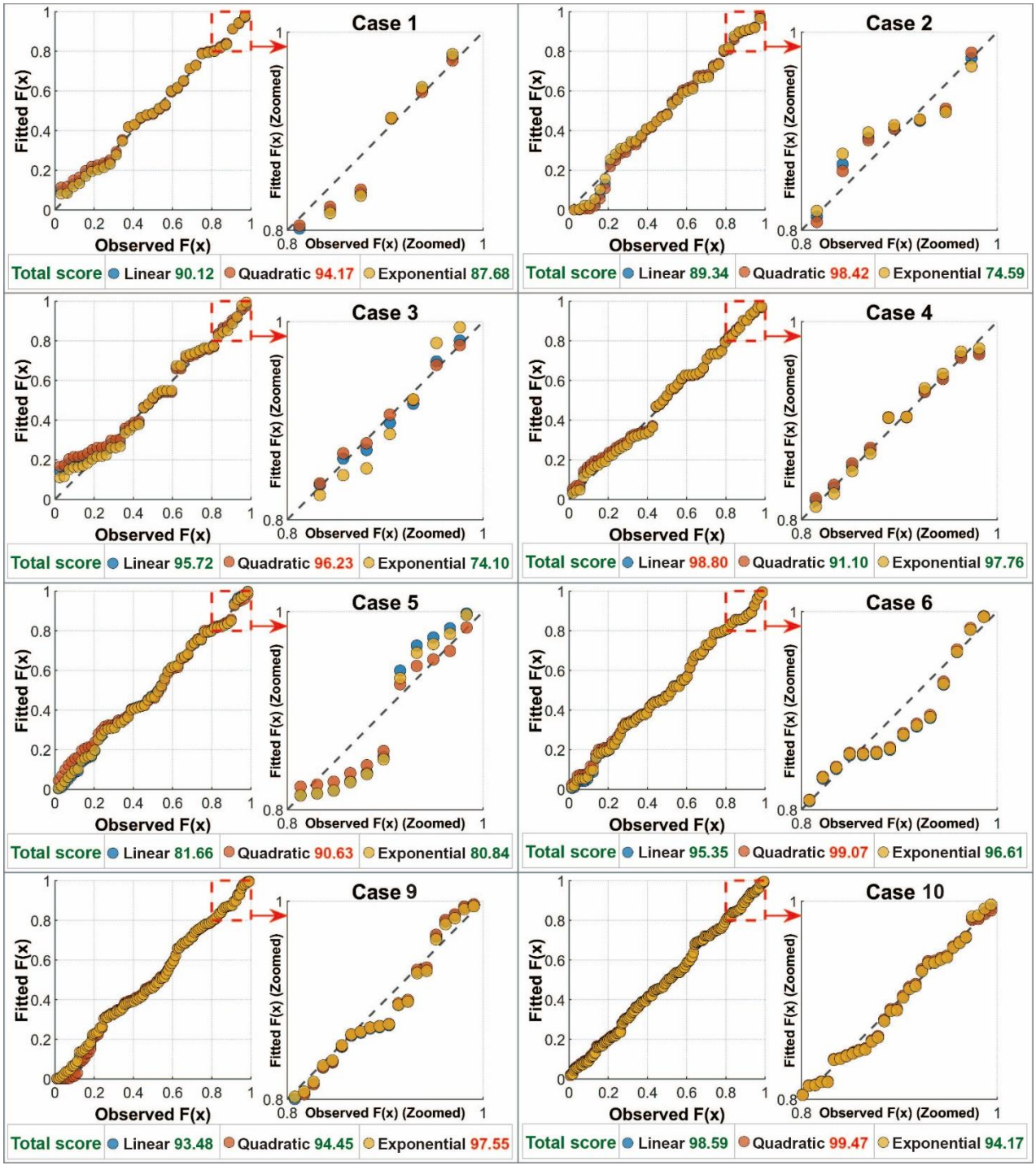

Figure 7: Comparison between TCEV distribution fitted and observed F(x) values across cases using three weighting schemes: linear (blue), quadratic (orange), and exponential (yellow). Each subplot shows the fitted vs. observed values, with the ideal 1:1 line shown for reference. The total score for each scheme is provided below its subplot. A detailed inset highlights the high-F(x) interval [0.8, 1].

https://doi.org/10.5194/egusphere-2026-2664
Preprint. Discussion started: 11 June 2026

In most cases, at least one of the optimal weighting scheme achieves full marks in the two intervals of [0.6, 0.8) and [0.8, 1.0]. The superior performance of the optimal scheme is particularly evident in the critical medium-to-high interval [0.6, 1.0]. In Fig. 7, the optimal fitted values within the zoomed-in [0.8, 1.0] interval are close to the diagonal line. This is clearly demonstrated in Fig. 6, where the darkest blue cells within this interval indicate the lowest RMSE values, highlighting the scheme's robustness in extreme value fitting, precisely the primary objective of this study. Notably, while the exponential weighting scheme achieved the best (lowest) overall RMSE across the entire distribution [0, 1.0] (as shown in the rightmost column of Fig. 6), its performance in the critical high-value range was often suboptimal (except Case 9). This indicates a trade-off where the exponential scheme provides a balanced global fit, but can sacrifice precision in the tail region that is most critical for extreme value analysis.

Our selection strategy prioritizes guaranteeing precision in the most critical interval ([0.8, 1.0]) first, and then seeks to extend robust performance to the interval ([0.6, 0.8)). This approach ensures a more balanced and reliable fit, rather than overfitting to either isolated extremes or the entire of the data. Notably, the optimal weighting scheme varies across cases, suggesting a potential influence of data distribution attributes. The potential mechanisms underlying these performance differences will be explored in Sect. 5.

4.3 Comparison of SR-MWS versus existing methods

To visually assess the fitting accuracy, Fig. 8 compares the RMSE of various fitting methods across different F(x) intervals for each case. The RMSE of the comparison methods (TCEV-IML, TCEV-MOF, and TCEV-MCS) exhibited significant fluctuations. For instance, while these methods showed relatively low RMSE in low-value intervals, their RMSE increased significantly as F(x) rose into the median interval such as [0.6, 0.8), indicating increased prediction errors and reduced accuracy. In contrast, the proposed SR-MWS method maintained low and stable RMSE values especially in medium-to-high intervals [0.6, 1.0]. This performance demonstrates the effectiveness of the SR-MWS weighting scheme, which better captures data characteristics, reduces prediction bias, and thus enhances right-tail prediction.

Next, we applied the partitioned scoring framework proposed in Sect. 2.3.4 to quantitatively evaluate the fitting performance from anothor perspective. The results for the different methods are presented in Fig. 9. The intersection point of the TCEV distribution fitted F(x) curve with a given return period line defines the estimated severity of an extreme event at that period. To facilitate clear demonstration and in-depth analysis, we utilized the transformation function $-\ln(-\ln(F(x)))$, which serves to accentuate the differences between methods in assessing this severity. In the figure, the intersection points vary across methods, indicating that the choice of fitting method directly influences the estimated severity of an extreme event. This has direct practical implications, as differing estimates affect decision-makers' judgment of event severity and consequently determine the scale and cost of flood control facilities in hydraulic engineering design. Therefore, selecting an appropriate fitting method is critical for accurate risk assessment and rational planning of engineering measures.

https://doi.org/10.5194/egusphere-2026-2664
Preprint. Discussion started: 11 June 2026

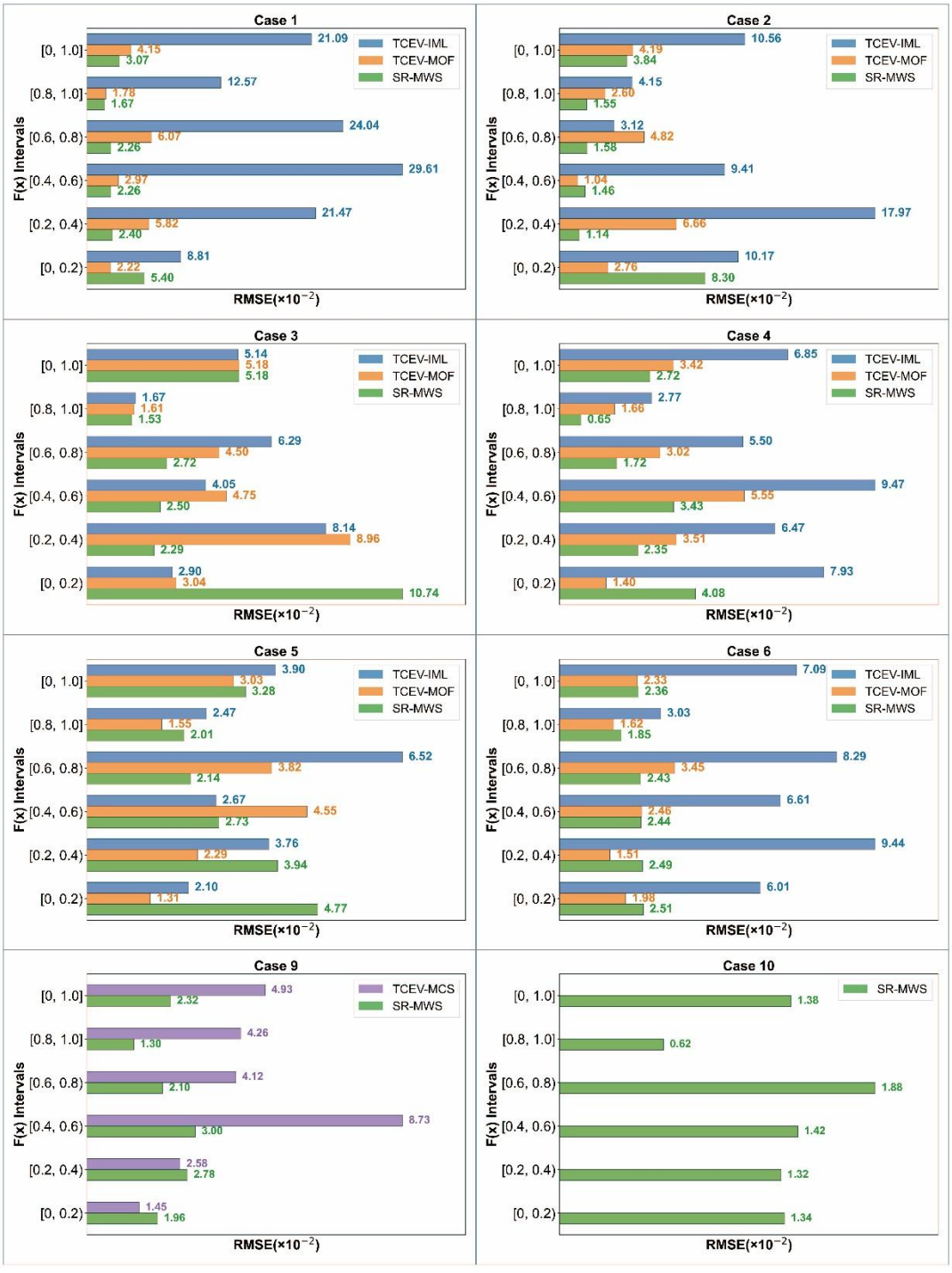

Figure 8: Comparison of RMSE across different methods across intervals of F(x). The bar chart compares the RMSE of four methods (TCEV-IML (blue), TCEV-MOF (orange), TCEV-MCS (purple), and SR-MWS (green)) over six intervals of the F(x): [0, 0.2), [0.2, 0.4), [0.4, 0.6), [0.6, 0.8), [0.8, 1.0] and the full range [0,1.0]. The vertical axis lists the F(x) intervals. The exact RMSE value is annotated above each bar.

https://doi.org/10.5194/egusphere-2026-2664
Preprint. Discussion started: 11 June 2026

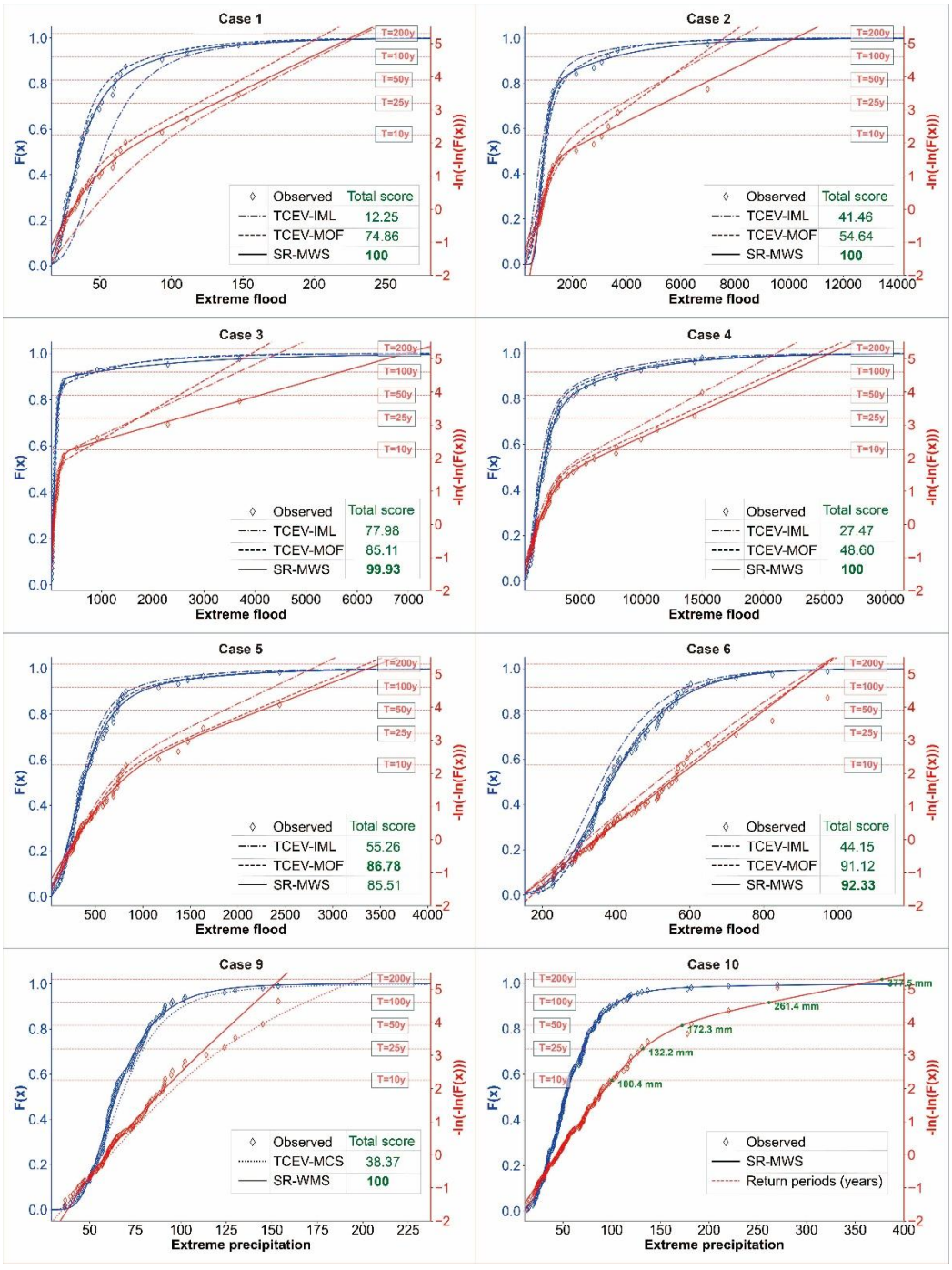

Figure 9: Comparison of F(x) fitting with different methods and return periods. The horizontal axis represents the intensity of extreme events. The blue vertical axis on the left corresponds to the F(x), and the red vertical axis on the right is the transformation function −ln(−ln(F(x))). The diamond symbols represent observed. The dash-dotted, dashed, dotted, and solid lines represent the fitting curves of the TCEV-IML, TCEV-MOF, TCEV-MCS and SR-MWS method, respectively. Red horizontal lines indicate different return periods, and the total score for each method is also annotated.

https://doi.org/10.5194/egusphere-2026-2664
Preprint. Discussion started: 11 June 2026

The proposed SR-MWS method consistently outperforms the other approaches across the tested cases. It achieves perfect scores (100 points) in Cases 1, 2, 4, and 9, and attains the highest total score in all cases except Case 5. This superior and stable performance is particularly evident in medium-to-high F(x) intervals, which are most relevant for extreme-event characterization, as well as in the overall assessment. These results demonstrate the robustness and reliability of SR-MWS for extreme-value analysis.

A detailed analysis of the successful application of SR-MWS to Case 10 is presented in Fig. 9. The TCEV distribution provides quantitative estimates of extreme precipitation for key return periods: 100.4 mm (10-year), 132.2 mm (25-year), 172.3 mm (50-year), 261.4 mm (100-year), and 377.5 mm (200-year). This clearly highlights the distribution's ability to simulate low-frequency extreme events. Notably, a sharp decline is observed in the probability for events exceeding approximately 130 mm, indicating that such events are relatively rare. These quantitative estimates, such as the precipitation corresponding to different return periods, provide crucial references for engineering design and disaster preparation. They help in understanding the potential scale of high-impact precipitation scenarios and in formulating appropriate strategies to reduce the associated risks.

For Case 5, we specifically analyzed the fitting residuals of SR-MWS and TCEV-MOF, as shown in Fig. 10. In the interval [0.9, 1] (red box), the residual of the SR-MWS method was relatively close to 0, indicating that SR-MWS fitted these extreme flood data better than TCEV-MOF. In contrast, the residual of TCEV-MOF in the interval [0.8, 0.9) (blue box) was relatively small, indicating better fitting performance in that region. This reveals differences in the adaptability of the two methods across different data intervals. Although SR-MWS did not exceed TCEV-MOF in terms of overall scores, its RMSE was within 0.005 (as shown in Fig. 8). The performance advantage of SR-MWS became more pronounced as events become more extreme, as evidenced by its superior performance in the high-value interval [0.9, 1.0]. This gives it a clear competitive edge over traditional methods in application scenarios that demand high predictive accuracy for extreme events.

https://doi.org/10.5194/egusphere-2026-2664
Preprint. Discussion started: 11 June 2026

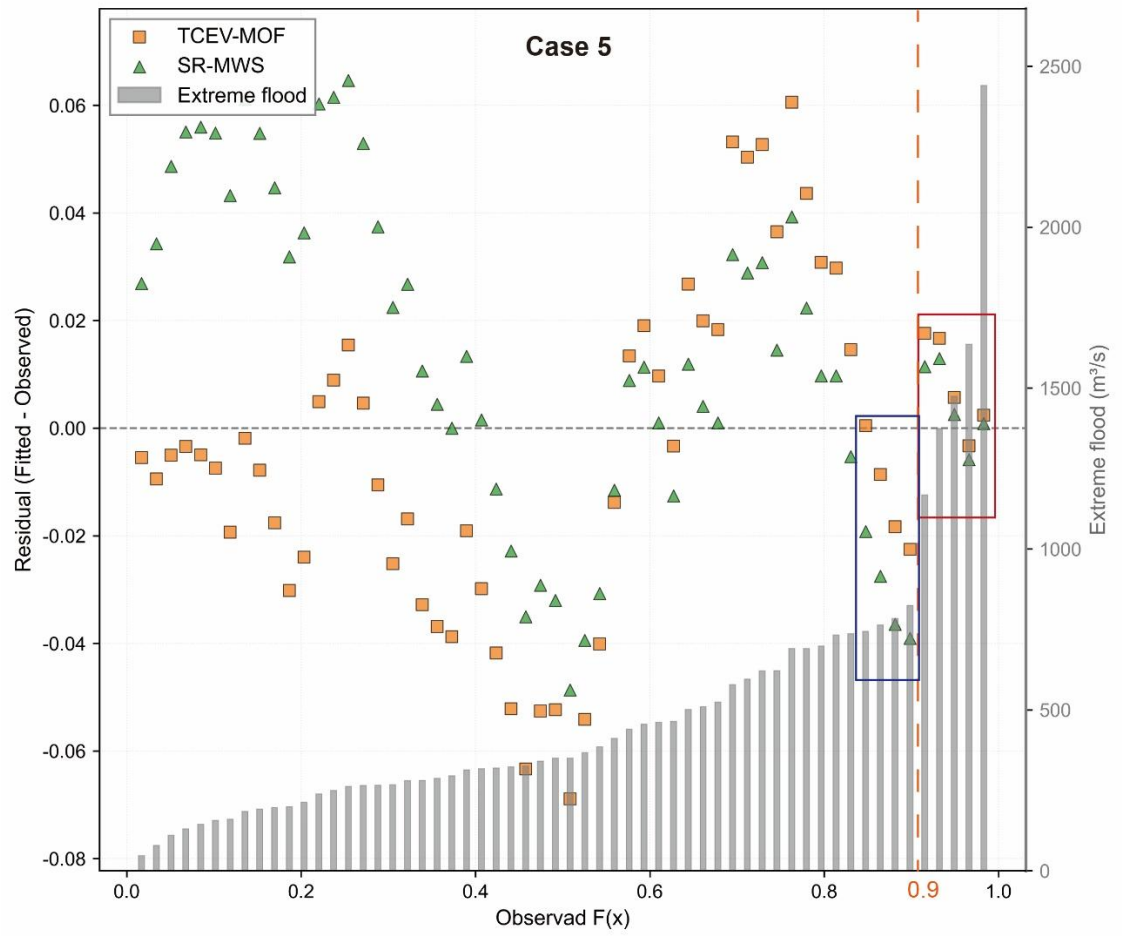

Figure 10: Residual analysis in Case 5 between TCEV-MOF and SR-MWS methods. The horizontal axis represents the F(x), and the left vertical axis shows the residual. Residuals are plotted as orange squares for TCEV-MOF and green triangles for SR-MWS. The histogram shows the corresponding extreme flood (m³/s) (right vertical axis) across the F(x) values. Boxes are used to highlight a clear performance difference between the methods.

4.4 Comparison of SR-MWS with benchmark methods

This section evaluates the performance of SR-MWS in comparison with representative benchmark methods from both global and tail perspectives. The global RMSE comparison of different methods is shown in Fig. 11. The results show that SR-MWS achieves the lowest median RMSE (0.025) and demonstrates the best overall fitting performance among all methods. The median RMSE of the GEV distribution is 0.031, while the Gumbel method shows a moderate level of performance (0.048). In contrast, the POT method exhibits significantly higher errors (0.079), reflecting its limitation in representing the full distribution due to its focus on threshold exceedances. In addition, the interquartile range of SR-MWS is more compact than other methods, indicating higher stability and robustness across different datasets. The POT method shows substantial variability, suggesting high sensitivity to data fluctuations when applied to full distribution fitting.

https://doi.org/10.5194/egusphere-2026-2664
Preprint. Discussion started: 11 June 2026

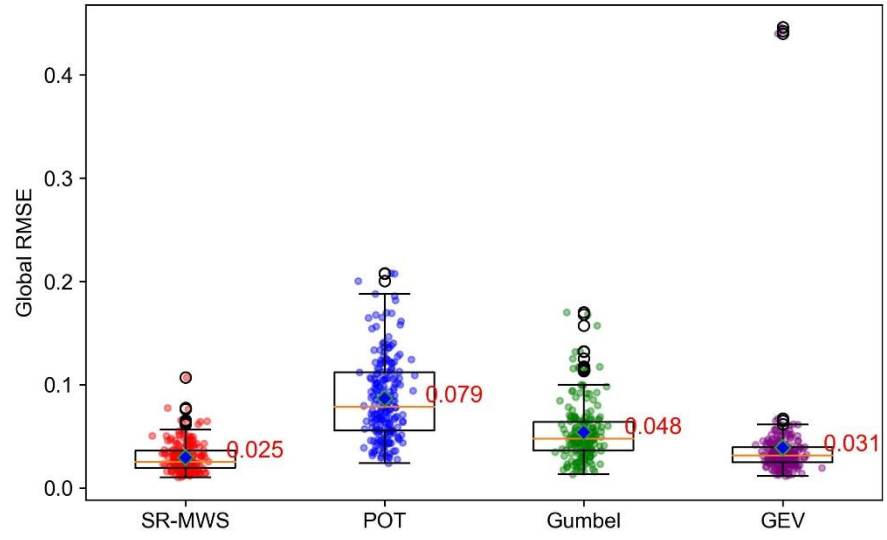

Figure 11: Global RMSE comparison of SR-MWS and benchmark methods based on simulated datasets.

The tail RMSE (F>0.8), which evaluates the ability of each method to capture extreme events, is illustrated in Fig. 12. Since the POT method is specifically designed to model exceedances, it achieves the lowest median tail RMSE (0.013), as expected. SR-MWS also demonstrates competitive tail performance (0.015), outperforming the GEV (0.021) and Gumbel (0.034). This indicates that SR-MWS can effectively capture extreme behaviour, even though it is not explicitly designed as a tail-focused method. In contrast, the Gumbel distribution performs the worst in the tail region, reflecting its limited flexibility in modeling heavy-tailed distributions.

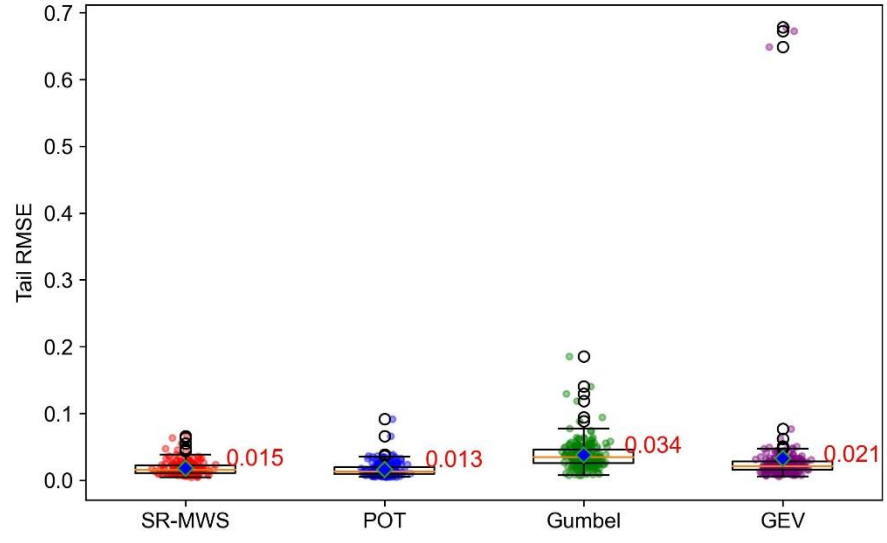

Figure 12: Tail RMSE comparison (F>0.8) of SR-MWS and benchmark methods based on simulated datasets.

https://doi.org/10.5194/egusphere-2026-2664
Preprint. Discussion started: 11 June 2026

The comparison results reveal a clear trade-off among the benchmark methods. The POT method performs well in tail modeling but is less effective in fitting the overall distribution. In contrast, the GEV and Gumbel methods provide more balanced performance, but struggle to accurately capture extreme events. SR-MWS, however, achieves strong performance in both global and tail evaluations. It outperforms all benchmark methods in overall fitting accuracy while maintaining tail performance comparable to that of the POT method. This suggests that SR-MWS effectively bridges the gap between full-distribution fitting and extreme value modeling.

The superior performance of SR-MWS can be attributed to its adaptive weighting mechanism, which increases the influence of extreme observations while slightly reducing the emphasis on ordinary events. As a result, the SR-MWS method provides a unified framework capable of modeling both typical and extreme hydrological behaviours.

5 Discussion

The SR-MWS method explicitly emphasizes right-tail information through an adaptive weighting strategy, resulting in improved performance in TCEV distribution assessment. Its fully automated workflow enables efficient processing of large data volumes without manual intervention, ensuring both objectivity and computational efficiency. This automation is particularly advantageous for extreme-event analysis, as it allows TCEV parameters to be updated in a timely and consistent manner, thereby supporting more reliable and responsive decision-making under extreme conditions.

The comparison results between simulated data and benchmark methods in Sect. 4.4 further highlight the effectiveness of the proposed framework. Specifically, SR-MWS achieves superior global fitting performance while maintaining tail accuracy comparable to the POT method. This indicates that the proposed approach effectively balances the long-standing trade-off between full distribution fitting and extreme value representation. Benchmark methods such as GEV and Gumbel provide reasonable overall fits but fail to adequately capture extreme events. Although the POT method performs well in tail modeling, it lacks the ability to characterize the complete distribution. In contrast, SR-MWS has successfully bridged the gap between global fitting and tail evaluation by constructing a unified framework that performs well in both.

The applicability of the TCEV distribution was assessed using the slope-ratio criterion R. Compared with the visual inspection approach adopted by Campos-Aranda (2021), this criterion offers a more consistent, objective, and reproducible means of evaluation. The threshold value of 1.5 adopted for the slope ratio is based on empirical experience and serves as a practical reference. Alternative threshold values may be considered in future applications depending on data characteristics and research objectives.

https://doi.org/10.5194/egusphere-2026-2664
Preprint. Discussion started: 11 June 2026

Based on the partitioned scoring framework, the optimal weighting scheme varies across cases, reflecting differences in right-tail generating mechanisms rather than arbitrary weighting choices. When extreme events are sparse, the right-tail exhibits pronounced curvature and separation from the bulk of the distribution, consistent with extremes arising from distinct generating processes. In such cases, stronger right-tail weighting is required to adequately constrain tail behaviour (Rossi et al., 1984; Coles et al., 2001). Conversely, when extreme events occur more frequently, the high-value region becomes smoother, indicating partial overlap between ordinary and extreme-event populations, for which more balanced weighting yields more stable estimation (Huser and Wadsworth, 2022; Villarini and Smith, 2010). When the transition from ordinary to extreme values is gradual, tail behaviour is already well constrained by the data, and additional weight amplification provides limited benefit (Katz et al., 2002; Bracken et al., 2018). The proposed SR-MWS method explicitly identifies these tail-structure differences and adaptively selects the weighting scheme accordingly.

Using the SR-MWS results for Case 10 as a baseline, systematic perturbations of the parameters α_2 and β_2 produce pronounced upward or downward shifts in the fitted TCEV distribution curves. This sensitivity is further illustrated by changes in the transformed function $-\ln(-\ln(F(x)))$ shown in Fig. 13, underscoring the importance of accurate optimization of α_2 and β_2. Among the two parameters, α_2 exerts a markedly stronger influence on extreme-value estimates. Decreasing α_2 leads to systematic overestimation of extremes. For instance, at a return period of 25 years, a 50% reduction in α_2 results in an estimated extreme precipitation value approximately twice the baseline. Conversely, increasing α_2 produces underestimation, with a 50% increase yielding an estimate roughly half of the baseline at a 200-year return period. Such sensitivity has direct implications for engineering applications, as misestimation of α_2 can lead either to overly conservative designs with unnecessary construction costs or to underestimated flood hazards that compromise risk assessment and management decisions.

In the context of increasing hydroclimatic variability, improving the robustness of extreme-value estimation remains a key challenge. The SR-MWS method addresses this challenge by adaptively accounting for differences in tail structure and generating mechanisms, thereby enhancing the reliability of extreme-event characterization. While demonstrated here for hydrological extremes, the general framework is applicable to other mixed-population problems exhibiting “dog-leg” behaviour, suggesting potential for broader use in extreme-value analysis.

https://doi.org/10.5194/egusphere-2026-2664
Preprint. Discussion started: 11 June 2026

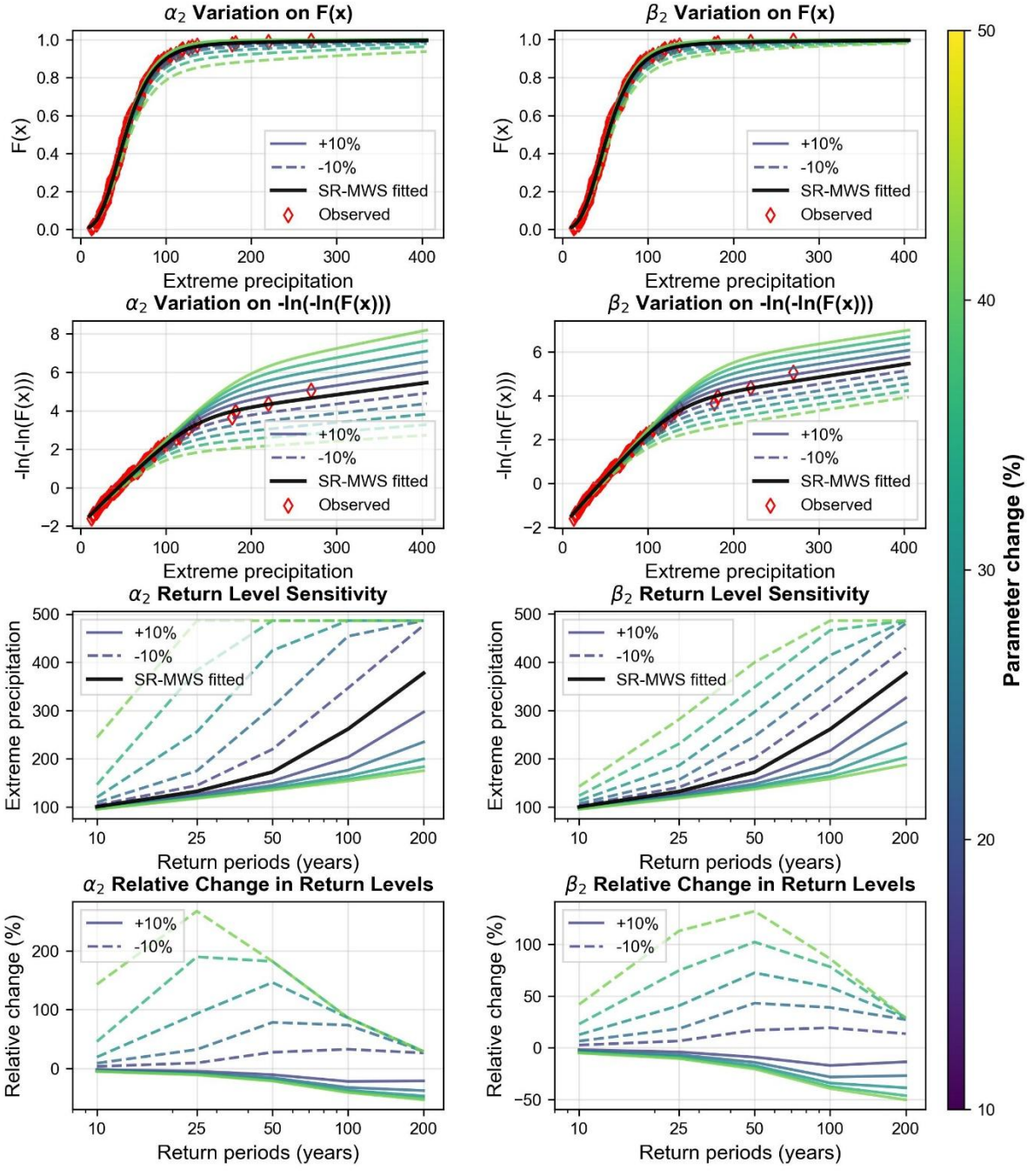

Figure 13: Parameter sensitivity analysis in Case 10. The left and right columns correspond to the analysis of parameters α_2 and β_2, respectively. Row 1 illustrates the impact of parameter variations on the F(x). The black solid line denotes the F(x) fitted using the SR-MWS method. The observed are marked by red diamond symbols. The solid and dashed lines, graded from dark to light, represent the F(x) curves when the parameter is increased by 10%, and decreased by 10% to 50%, respectively. Row 2 demonstrates the impact of parameter variations on the transformed function −ln(−ln(F(x))). Row 3 presents the sensitivity of the return level to parameter changes. Row 4 shows the relative change in the return level resulting from parameter changes.

https://doi.org/10.5194/egusphere-2026-2664
Preprint. Discussion started: 11 June 2026

6 Conclusions

This study develops an objective and fully automated SR-MWS framework for fitting the TCEV distribution, with the explicit aim of improving the reliability of extreme-value estimation in hydrological applications. By integrating a partitioned scoring framework with adaptive weighting, SR-MWS systematically identifies the weighting strategy that best reflects right-tail behaviour, thereby reducing subjectivity and enhancing both accuracy and robustness in extreme-event prediction.

The proposed method further provides a consistent workflow for assessing data suitability for the TCEV distribution and for initializing model parameters, ensuring stable and reproducible results across diverse cases. The results from both hydrological datasets and simulated experiments demonstrate that the proposed SR-MWS framework provides a robust and generalizable approach for extreme-value modeling. These advantages make SR-MWS a practical and efficient tool for applications such as hydrological design, safety evaluation, and risk-informed decision-making.

Beyond hydrological extremes, the methodological principles of SR-MWS are not restricted to a specific hazard type. The framework is applicable to a broad class of extreme-value problems exhibiting “dog-leg” or mixed-population characteristics, providing a transferable solution for multidisciplinary extreme-value analysis. To facilitate transparency, reproducibility, and further development, the complete workflow is made publicly available through open-source code, enabling straightforward adoption by both researchers and practitioners.

Code and data availability

The MATLAB codes developed in this study are publicly available at https://github.com/Liangyu2021/TCEV-SR-MWS.git.

Author contributions

Liangyu Ta: Conceptualization, Method, Formal analysis, Data curation, Validation, Writing – original draft, Writing – review and editing. Javier Valdes-Abellan: Conceptualization, Method, Writing – review and editing, Supervision. Chen Yu: Conceptualization, Method, Resources, Funding acquisition, Writing – review and editing. Zhenhong Li: Conceptualization, Method, Writing – review and editing.

Competing interests

The contact author has declared that none of the authors has any competing interests.

https://doi.org/10.5194/egusphere-2026-2664
Preprint. Discussion started: 11 June 2026

Disclaimer

Publisher's note: Copernicus Publications remains neutral with regard to jurisdictional claims made in the text, published maps, institutional affiliations, or any other geographical representation in this paper. The authors bear the ultimate responsibility for providing appropriate place names. Views expressed in the text are those of the authors and do not necessarily reflect the views of the publisher.

Financial support

This research was funded by the National Science and Technology Major Project (2024ZD1000407), the National Natural Science Foundation of China (42377159), the Shaanxi Province Science and Technology Innovation Team (2021TD-51), the Shaanxi Province Geoscience Big Data and Geohazard Prevention Innovation Team (2022), and the Fundamental Research Funds for the Central Universities, CHD (300102263401). This research was supported by a Chinese Scholarship Council studentship awarded to Liangyu Ta (Ref. 202406560163). Gratitude is also expressed to the Spanish National Agency of Meteorology which provided some datasets included in the present study.

References

Aranda, D. F. C.: Hacia el enfoque global en el análisis de frecuencia de crecientes, Tecnología y ciencias del agua, 14, 23-42, 1999.

Beven, K. and Binley, A.: The future of distributed models: Model calibration and uncertainty prediction, Hydrological Processes, 6, 279-298, https://doi.org/10.1002/hyp.3360060305, 1992.

Blom, G.: Statistical estimates and transformed beta-variables, Almqvist & Wiksell, 1958.

Boni, G., Parodi, A., and Rudari, R.: Extreme rainfall events: Learning from raingauge time series, Journal of Hydrology, 327, 304-314, https://doi.org/10.1016/j.jhydrol.2005.11.050, 2006.

Bracken, C., Holman, K. D., Rajagopalan, B., and Moradkhani, H.: A Bayesian Hierarchical Approach to Multivariate Nonstationary Hydrologic Frequency Analysis, Water Resources Research, 54, 243-255, https://doi.org/10.1002/2017WR020403, 2018.

Campos-Aranda, D. F.: Ajuste de la distribución de valores extremos de dos componentes (TCEV) por medio de máxima verosimilitud, Tecnología y ciencias del agua, 12, 442-489, https://doi.org/10.24850/j-tyca-2021-02-10, 2021.

Cannarozzo, M., D'Asaro, F., and Ferro, V.: Regional rainfall and flood frequency analysis for Sicily using the two component extreme value distribution, Hydrological Sciences Journal, 40, 19-42, https://doi.org/10.1080/02626669509491388, 1995.

Clarke, R. T.: Estimating time trends in Gumbel-distributed data by means of generalized linear models, Water Resources Research, 38, 16-11-16-11, https://doi.org/10.1029/2001WR000917, 2002.

https://doi.org/10.5194/egusphere-2026-2664
Preprint. Discussion started: 11 June 2026

Coles, S., Bawa, J., Trenner, L., and Dorazio, P.: An introduction to statistical modeling of extreme values, Springer, 2001.

Cunnane, C.: Unbiased plotting positions — A review, Journal of Hydrology, 37, 205-222, https://doi.org/10.1016/0022-1694(78)90017-3, 1978.

Davison, A. C. and Smith, R. L.: Models for exceedances over high thresholds, Journal of the Royal Statistical Society Series B: Statistical Methodology, 52, 393-425, https://doi.org/10.1111/j.2517-6161.1990.tb01796.x, 1990.

De Luca, D. L. and Napolitano, F.: A user-friendly software for modelling extreme values: EXTRASTAR (EXTRemes Abacus for STAtistical Regionalization), Environmental Modelling & Software, 161, 105622, https://doi.org/10.1016/j.envsoft.2023.105622, 2023.

De Luca, D. L., Ridolfi, E., Russo, F., Moccia, B., and Napolitano, F.: Climate change effects on rainfall extreme value distribution: the role of skewness, Journal of Hydrology, 634, 130958, https://doi.org/10.1016/j.jhydrol.2024.130958, 2024.

Escalante-Sandoval, C. and Reyes-Chávez, L.: Análisis bivariado de gastos máximos anuales con distribuciones marginales TCEV, XVIII Congreso Nacional de Hidráulica, 523-529, 2004.

Etoh, T., Murota, A., and Nakanishi, M.: SQRT-exponential type distribution of maximum, Hydrologic Frequency Modeling, Dordrecht, 1987//, 253-264, https://doi.org/10.1007/978-94-009-3953-0_17,

Ferro, V. and Porto, P.: Flood frequency analysis for Sicily, Italy, Journal of Hydrologic Engineering, 11, 110-122, https://doi.org/10.1061/(ASCE)1084-0699(2006)11:2(110), 2006.

Fiorentino, M., Arora, K., and Singh, V. P.: The two-component extreme value distribution for flood frequency analysis: Derivation of a new estimation method, Stochastic Hydrology and Hydraulics, 1, 199-208, https://doi.org/10.1007/BF01543891, 1987.

Fowler, H. J., Lenderink, G., Prein, A. F., Westra, S., Allan, R. P., Ban, N., Barbero, R., Berg, P., Blenkinsop, S., Do, H. X., Guerreiro, S., Haerter, J. O., Kendon, E. J., Lewis, E., Schaer, C., Sharma, A., Villarini, G., Wasko, C., and Zhang, X.: Anthropogenic intensification of short-duration rainfall extremes, Nature Reviews Earth & Environment, 2, 107-122, https://doi.org/10.1038/s43017-020-00128-6, 2021.

Francés, F.: Utilización de la Información Histórica en el Análisis Regional de las Avenidas, Monografia CIMNE, 27, 1995.

Francés, F.: Using the TCEV distribution function with systematic and non-systematic data in a regional flood frequency analysis, Stochastic Hydrology and Hydraulics, 12, 267-283, https://doi.org/10.1007/s004770050021, 1998.

Fuller Weston, E.: Flood flows, Transactions of the American Society of Civil Engineers, 77, 564-617, https://doi.org/10.1061/taceat.0002552, 1914.

Galvez-Hernandez, P., Dai, Y., and Muntaner, C.: The DANA disaster: Unraveling the political and economic determinants for Valencia's floods devastation, International Journal for Equity in Health, 24, 64, https://doi.org/10.1186/s12939-025-02435-0, 2025.

Gómez, J., Aparicio, J., and Patiño, C.: Manual de análisis de frecuencias en hidrología, México: Instituto Mexicano de Tecnología del Agua, 2010.

https://doi.org/10.5194/egusphere-2026-2664
Preprint. Discussion started: 11 June 2026

Gringorten, I. I.: A plotting rule for extreme probability paper, Journal of Geophysical Research (1896-1977), 68, 813-814, https://doi.org/10.1029/JZ068i003p00813, 1963.

Gumbel, E. J.: The return period of flood flows, The Annals of Mathematical Statistics, 12, 163-190, https://doi.org/10.1214/aoms/1177731747, 1941.

Gumbel, E. J.: Statistics of extremes, Courier Corporation, 2004.

Haan, C. T., Barfield, B. J., and Hayes, J. C.: Design hydrology and sedimentology for small catchments, Elsevier, 1994.

Hazen, A.: Storage to be provided in impounding municipal water supply, Transactions of the American Society of Civil Engineers, 77, 1539-1640, https://doi.org/10.1061/taceat.0002563, 1914.

Helsel, D. R. and Hirsch, R. M.: Statistical methods in water resources techniques of water resources investigations, Book 4, chapter A3. U.S. Geological Survey, Elsevier, 2002.

Huser, R. and Wadsworth, J. L.: Advances in statistical modeling of spatial extremes, WIREs Computational Statistics, 14, e1537, https://doi.org/10.1002/wics.1537, 2022.

Katz, R. W., Parlange, M. B., and Naveau, P.: Statistics of extremes in hydrology, Advances in Water Resources, 25, 1287-1304, https://doi.org/10.1016/S0309-1708(02)00056-8, 2002.

Kottegoda, N. T. and Rosso, R.: Applied statistics for civil and environmental engineers, Blackwell Publishing Ltd, UK, 2008.

Mahmood, M. I., Elagib, N. A., Horn, F., and Saad, S. A.: Lessons learned from Khartoum flash flood impacts: An integrated assessment, Science of the Total Environment, 601, 1031-1045, https://doi.org/10.1016/j.scitotenv.2017.05.260, 2017.

Matalas, N. C., Slack, J. R., and Wallis, J. R.: Regional skew in search of a parent, Water Resources Research, 11, 815-826, https://doi.org/10.1029/WR011i006p00815, 1975.

Merz, R. and Blöschl, G.: Flood frequency hydrology: 1. Temporal, spatial, and causal expansion of information, Water Resources Research, 44, https://doi.org/10.1029/2007WR006744, 2008.

Molina-Aguilar, J. P., Gutiérrez-López, M. A., and Aparicio-Mijares, F. J.: Búsqueda armónica para optimizar la función Gumbel Mixta univariada, Tecnología y ciencias del agua, 9, 280-322, https://doi.org/10.24850/j-tyca-2018-05-11, 2018.

Moustakis, Y., Papalexiou, S. M., Onof, C. J., and Paschalis, A.: Seasonality, intensity, and duration of rainfall extremes change in a warmer climate, Earth's Future, 9, e2020EF001824, https://doi.org/10.1029/2020EF001824, 2021.

Papalexiou, S. M. and Montanari, A.: Global and regional increase of precipitation extremes under global warming, Water Resources Research, 55, 4901-4914, https://doi.org/10.1029/2018WR024067, 2019.

Pickands, J.: Statistical inference using extreme order statistics, The Annals of Statistics, 3, 119-131, 1975.

Potter, W. D.: Upper and lower frequency curves for peak rates of runoff, Eos, Transactions American Geophysical Union, 39, 100-105, https://doi.org/10.1029/TR039i001p00100, 1958.

Rentschler, J., Salhab, M., and Jafino, B. A.: Flood exposure and poverty in 188 countries, Nat Commun, 13, 3527, https://doi.org/10.1038/s41467-022-30727-4, 2022.

https://doi.org/10.5194/egusphere-2026-2664
Preprint. Discussion started: 11 June 2026

Rosenbrock, H. H.: An automatic method for finding the greatest or least value of a function, The Computer Journal, 3, 175-184, https://doi.org/10.1093/comjnl/3.3.175, 1960.

Rossi, F., Fiorentino, M., and Versace, P.: Two-component extreme value distribution for flood frequency analysis, Water Resources Research, 20, 847-856, https://doi.org/10.1029/WR020i007p00847, 1984.

Senent-Aparicio, J., López-Ballesteros, A., Jimeno-Sáez, P., and Pérez-Sánchez, J.: Recent precipitation trends in Peninsular Spain and implications for water infrastructure design, Journal of Hydrology: Regional Studies, 45, 101308, https://doi.org/10.1016/j.ejrh.2022.101308, 2023.

Stedinger, J. R., Vogel, R. M., and Foufoula-Georgiou, E.: Frequency analysis of extreme events, in: Handbook of Hydrology, edited by: Maidment, D., McGraw-Hill, N. Y (chap. 18), 1993.

Valdes-Abellan, J., Pla, C., Fernandez-Mejuto, M., and Andreu, J. M.: Validating the KAGIS black-box GIS-based model in a Mediterranean karst aquifer: Case of study of Mela aquifer (SE Spain), Hydrological Processes, 32, 2584-2596, https://doi.org/10.1002/hyp.13215, 2018.

Villarini, G. and Smith, J. A.: Flood peak distributions for the eastern United States, Water Resources Research, 46, https://doi.org/10.1029/2009WR008395, 2010.

Vogel Richard, M. and Wilson, I.: Probability Distribution of Annual Maximum, Mean, and Minimum Streamflows in the United States, Journal of Hydrologic Engineering, 1, 69-76, https://doi.org/10.1061/(ASCE)1084-0699(1996)1:2(69), 1996.

Weibull, W.: A statistical theory of strength of materials, Generalstabens Litografiska Anstalts Förlag, Stockholm, 1939.

Wojtczak, E., Rucka, M., and Andrzejewska, A.: Damage detection in 3D printed plates using ultrasonic wave propagation supported with weighted root mean square calculation and wavefield curvature imaging, Journal of Physics: Conference Series, 2647, 182003, https://doi.org/10.1088/1742-6596/2647/18/182003, 2024.

Wojtczak, E., Rucka, M., and Knak, M.: Detection and imaging of debonding in adhesive joints of concrete beams strengthened with steel plates using guided waves and weighted root mean square, Materials, 13, 2167, https://doi.org/10.3390/ma13092167, 2020.